Agr. Nat. Resour. 56 (2022) 957–970

AGRICULTURE AND NATURAL RESOURCES

Journal homepage: http://anres.kasetsart.org

Research article

Development of mangosteen peel ash as a heterogeneous catalyst for palm oil-derived fatty acid methyl ester production

Napaphat Kongrit[a], Issara Chanakaewsomboon[b], Jakkrapong Jitjamnong[a,*], Apanee Luengnaruemitchai[c], Naparat Kasetsomboon[d], Narinphop Chuaykarn[e], Chatrawee Direksilp[c], Nonlapan Khantikulanon[f], Chin Kui Cheng[g]

[a] *Department of Industrial Technology, Faculty of Industrial Education and Technology, Rajamangala University of Technology Srivijaya, Songkhla 90000, Thailand*

[b] *Faculty of Environmental Management, Prince of Songkla University, Songkhla 90110, Thailand*

[c] *The Petroleum and Petrochemical College, Chulalongkorn University, Bangkok 10330, Thailand*

[d] *School of Energy and Power Engineering, Jiangsu University, Jiangsu 212013, China*

[e] *Department of Food and Nutrition, Faculty of Liberal Arts, Rajamangala University of Technology Srivijaya, Songkhla 90000, Thailand*

[f] *Department of Environmental Health, Faculty of Public Health, Valaya Alongkorn Rajabhat University, Pathum Thani 13180, Thailand*

[g] *Center for Catalysis and Separation, Department of Chemical Engineering, College of Engineering, Khalifa University, Abu Dhabi 127788, United Arab Emirates*

Article Info

Article history:
Received 25 March 2022
Revised 19 July 2022
Accepted 31 July 2022
Available online 12 October 2022

Keywords:
Biodiesel,
Fatty acid methyl ester,
Heterogeneous catalyst,
Response surface methodology,
Transesterification

Abstract

Importance of the work: A solid carbon catalyst was derived from mangosteen peel ash (MA) activated by potassium hydroxide and used as a support for potassium carbonate (K_2CO_3). It was prepared as a heterogeneous catalyst for the transesterification of palm oil to fatty acid methyl esters.

Objectives: A central composite response surface methodology was used to optimize the biodiesel yield. The effects were investigated of different K_2CO_3 impregnation levels on MA (0 by weight percentage (wt.%), 25 wt.%, 30 wt.% and 35 wt.%) and then on the catalyst loading (2.32–5.68 wt.%), the methanol-to-oil molar ratio (3.95:1–14.05:1), and the reaction time (39.55–140.45 min) of the transesterification reaction at 65 °C.

Materials & Methods: The mangosteen peel was procured from Songkhla province, Thailand and the palm oil was purchased from a local supermarket in Songkhla province. The catalysts were prepared using the incipient wetness impregnation method and applied for transesterification of palm oil with methanol to produce biodiesel. The reaction process was optimized in terms of the biodiesel yield using response surface methodology based on a central composite design.

Results: The results demonstrated that the catalyst consisting of 30 wt.% K_2CO_3 loaded MA (30K-MA) had the highest catalytic activity. Using the 30K-MA catalyst at 65 °C, the maximum biodiesel yield of 97.9% was prodcued at a catalyst loading of 4.5 wt.%, a methanol-to-oil molar ratio of 10.8:1 and a reaction time of 98.7 min.

Main finding: The 30K-MA catalyst maintained sufficient catalytic activity (above 65% biodiesel yield) until the fourth reaction cycle, demonstrating the possibility of developing heterogeneous alkali catalysts from MA for biodiesel production.

* Corresponding author.
E-mail address: Jakkrapong.j@rmutsv.ac.th (J. Jitjamnong)

https://doi.org/10.34044/j.anres.2022.56.5.10

Introduction

Biodiesel, as a green fuel comprised of fatty acid alkyl esters, can be produced via transesterification from vegetable oils or animal fats with a low molecular weight alcohol in the presence of catalyst. Nowadays, biodiesel has been considered as an alternative source of energy, since it is a renewable and sustainable resource, clean burning, and non-toxic, with a higher flash point and cetane number, and more environmental friendly, where, upon combustion, it has lower emissions of carbon dioxide (CO_2), carbon monoxide (CO), sulfur oxides and nitrogen oxides than diesel fuel, and it is acceptable in current diesel engines without modification (Upretym et al., 2016; Abdullah et al., 2017; Changmai et al., 2020; Cong et al., 2020; Dubey et al., 2020).

The catalyst for transesterification reactions can be either basic or acid homogeneous or heterogeneous catalysts. Homogeneous basic catalysts, such as potassium hydroxide (KOH), sodium hydroxide, and sodium methoxide have the drawback of a lack of reusability, difficulty in the separation and purification of the catalyst from the products, and they produce a lot of alkali-contaminated wastewater (about 10% of the product volume) that imposes an additional operation cost of water treatment prior to discharge.Homogeneous acid catalysts, such sulfuric acid, phosphoric acid and hydrochloric acid, share the same problems as the basic catalysts mentioned above, plus they lead to serious environmental and corrosion problems (Abdullah et al., 2017; Chingakham et al., 2019). Therefore, solid-supported heterogeneous catalysts could be promising for more economical biodiesel production because of the easy separation of the catalyst from the product and their potential reusability (Tang et al., 2018; Arumugam and Sankaranarayanan, 2020; Chua et al., 2020).

Sustainable development has been promoted by the use of ash or biochar derived from waste material as a heterogeneous catalyst for biodiesel production because the as-prepared biochar or ash from biomass has a high carbon content and is obtained as the residual byproduct from the pyrolysis, gasification or hydrothermal carbonization of waste biomass (Bastos et al., 2020). It has been considered as an inexpensive and environmentally sound support for metal catalysts. However, as-prepared biochar or ash has poor physicochemical properties. Consequently, it has been improved by various activation and functionalization approaches, including activation with different potassium carbonate (K_2CO_3) loading levels followed by decomposition of K_2CO_3 to form potassium oxide (K_2O), which is thought to become the active component of the solid catalyst. (Cao et al., 2017; Wang et al., 2017; Zhao et al., 2018). Mangosteen (*Garcinia mangostana* L.) fruit is found throughout Southeast Asian countries, especially in Thailand, Malaysia and Indonesia. In Thailand, mangosteen is well known as the 'queen of fruit' due to its pleasant taste; in 2017, the total global production of mangosteen was approximately 700,000 t (Aizat et al., 2019); however, 1 kg of harvested mangosteen produces approximately 600 g of waste as mangosteen peel (Foo and Hameed, 2012; Nasrullah et al., 2019), which can cause environmental problems on disposal. As an alternative to disposal, mangosteen peel waste can be used as a renewable, low cost and abundant biomass for biochar or ash production. Accordingly, there have been a few studies on the use of activated carbon derived from waste mangosteen peel in several applications, such as contaminant removal (Ahmad and Alrozi, 2010; Foo and Hameed, 2012; Nasrullah et al., 2019), porous carbon for lithium-sulfur batteries (Xue et al., 2017), adsorbents for CO_2 capture (Li et al., 2018) and carbon dots (Yang et al., 2017). The use of mangosteen peel ash (MA) as a precursor was chosen in the current study due to its suitable chemical composition, with a typical content of carbon (62.7 weight percentage, wt.%), oxygen (28.8 wt.%), hydrogen (2.6 wt.%), nitrogen (5.8 wt.%) and sulfur (0.1 wt.%), according to Foo and Hameed (2012). However, the use of MA as a support for alkali metal heterogeneous catalysts for biodiesel production has not been reported.

Thus, in the current study, the optimization of MA was evaluated with various K_2CO_3 loading levels as a heterogeneous catalyst using response surface methodology (RSM) for biodiesel production, as fatty acid methyl esters, via transesterification of palm oil with methanol. RSM was chosen because it has been reported to optimize the interaction effects of the parameters for biodiesel production to achieve a maximal biodiesel conversion level. A central composite design (CCD) using RSM is appropriate for fitting a quadratic model as it helps to reduce the number of experimental runs (Ahmad and Alrozi, 2010). Indeed, RSM has been used for the optimization of waste-material-derived solid catalysts for biodiesel synthesis, such as from chicken egg shell (Tshizanga et al., 2017; Pandit and Fulekar, 2019; Jitjamnong et al., 2019), waste date pits (Abu-Jrai et al., 2017), murumuru kernel shell (Bastos et al., 2020), spent coffee grounds (Nguyen et al., 2020), sugarcane leaf ash (Arumugam and Sankaranarayanan, 2020), banana peduncles (Balajii and Niju, 2019,2020), waste cupuaçu (*Theobroma grandiflorum*) seeds (Mendonça et al., 2019a), banana peels (Betiku et al., 2016; Jitjamnong et al., 2020a, b) and lucky nut (Adepoju et al., 2018).

Therefore, the use of waste-material could have a large impact on biodiesel synthesis.

The focus of this research was to develop a heterogeneous catalyst derived from MA for the transesterification reaction of palm oil with methanol. The prepared catalyst was examined using X-ray diffractometry (XRD), scanning electron microscopy coupled with energy dispersive spectroscopy, Fourier-transform infrared (FTIR) spectroscopy, X-ray photoelectron spectroscopy (XPS), nitrogen (N_2) adsorption/desorption isotherms based on Brunauer-Emmett-Teller (BET) and Hammett indicator analyses. The reaction process was optimized in terms of the biodiesel yield using RSM based on a CCD. The effects were tested of the catalyst preparation K_2CO_3 loading level on MA and reaction conditions (methanol-to-oil molar ratio, catalyst loading and reaction time).

Materials and Methods

Materials

The mangosteen peel used in this study was procured in Songkhla province, Thailand and the palm oil was purchased from a local supermarket, Thailand. The physicochemical properties of the feed palm oil (density, viscosity, carbon residue and chemical composition) are shown in Table 1. The methanol (99.5%), sodium sulfate anhydrous (99%), KOH (85%), n-heptane and K_2CO_3 (99%) used in this study were all of analytical grade.

Table 1 Physiochemical properties of feed palm oil

Property	Unit	Value
Density at 15 °C	g/cm^3	0.92
Viscosity at 40 °C	mm^2/s	40.84
Carbon residue	wt.%	0.38
Free fatty acid	wt.%	-[a]
Triglyceride (%)	wt.%	97.94±0.18
Diglyceride (%)	wt.%	2.30±0.18
Monoglyceride (%)	wt.%	-[a]
Ester	wt.%	-[a]

wt.% = weight percentage; [a] = not detected

Preparation of K_2CO_3/MA catalysts

The mangosteen peel was washed with distilled water to remove the impurities from the surface. The peel was dried in an oven at 105 °C for 24 h, pulverized and then sieved to obtain particles of size ≤ 1 mm. After that, the samples were calcined at 600 °C for 2 h to generate the MA. The prepared catalyst activation method was adopted from Zhao et al. (Zhao et al., 2018). The obtained MA was activated in 2 M KOH solution with stirring for 2 h. Then, the mixture was filtered and washed with distilled water until the pH of filtrate was 7. The obtained MA was dried in an oven at 105 °C overnight and then mixed with K_2CO_3 using the wet impregnation method. The loading level of the solution of K_2CO_3 was varied in the range 25–35 wt.%. In a typical process, to prepare a catalyst with a 25 wt.% K_2CO_3 loading (25K-MA), 2.5 g of K_2CO_3 powder was dissolved in distillate water and 7.5 g of dried MA was added and mixed with stirring at 600 revolutions per minute (rpm) for 2 h. After that, the sample was dried in an oven at 105 °C for 24 h and then calcined at 600 °C under atmospheric pressure for 4 h. The catalysts were labelled as αK-MA, where α represents the K_2CO_3 loading level (as a weight percentage).

Catalyst characterization

The basicity of each catalyst was characterized using the conventional Hammett indicator method based on titration with benzoic acid (0.01 M). The indicators were: bromothymol blue (H_- = 7.2), phenolphthalein (H_- = 9.8), 2,4-dinitroaniline (H_- = 15.0) and 4-nitroaniline (H_- = 18.4). The titration method measured the total basic sites of each catalyst.

The morphology and actual elements on the surface of the catalysts were observed using SEM (Oxford Aztec model) equipped with an energy dispersive X-ray spectroscopy (EDS) detector at an accelerating voltage of 2.0 kV and 1,000× magnification. The samples were mounted on a stub and then coated with platinum in a sputtering device before being placed in the sample holder of the SEM. The electron beam struck atoms on the surface of the sample to emit secondary electrons that then struck the detector to record the signals.

The textural properties (surface area) of the prepared catalyst were identified based on N_2 adsorption-desorption isotherms using Quantachrome Autosorb-1 MP surface area analyzer equipment and BET analysis over the pressure range of the ratio of absolute pressure to the saturation vapor pressure (P/P_0) of 0.05–0.3. Prior to performing the test, the volatile species that adsorbed on the catalyst surface were eliminated by heating the finely-powdered catalyst under vacuum conditions at 250 °C for 12–16 h. Helium gas was used as an adsorbate for blank analysis and nitrogen gas was used as an adsorbate for the actual analysis. The specific surface area (S_{BET}) of the catalyst was calculated using the the multi-point BET method.

The chemical functional groups of the prepared catalyst were examined using FTIR analysis with a Thermo Scientific, Nicolet iS5 FTIR spectrometer over a wavenumber range of 4000–650 cm^{-1}, with 64 scans and with a resolution of 4 cm^{-1} at room temperature. Each pellet was prepared from the mixture of a prepared catalyst and KBr powder.

The chemical composition of the catalysts was characterized using XRD analysis. The wide-angle X-ray diffraction patterns were recorded on a Rigaku X-ray diffractometer. The finely powdered catalyst was placed on a glass sample holder, which was then set at the center of the diffractometer to record the XRD profile over a 2θ range of 10–90° at a scanning speed of 5°/s and step size of 0.02°. The Cu-Kα radiation wavelength of 0.15406 nm was used as an X-ray source and operated in a ceramic X-ray tube at 40 kV/30 mA measurement. The obtained XRD patterns were compared to the standard file to identify the crystalline phases of the catalysts.

The chemical environments of the prepared catalysts were characterized using an XPS Kratos Axis Ultra DLD photoelectron spectrometer equipped with a magnetic immersion lens and charge neutralizer. The sample was examined using monochromatic an Al-Kα radiation source under a high vacuum condition (less than 5×10^{-7} torr) at 15 kV. The recorded spectra were calibrated based on the binding energy (BE) based on the C 1s spectral band at 284.6 eV from adventitious carbon. The Casa XPS software was used for the interpretation of the XPS spectra.

Experimental design for transesterification and statistical analysis using response surface methodology

A CCD was used to determine the optimization studies, with three parameters (catalyst loading, methanol-to-palm oil molar ratio and reaction time), five levels (-2, -1, 0, +1 and +2) and six replicate points at the central point (0, 0, 0). The total number of experimental runs was 20. The coded independent parameters are shown in Table 2.

The predicted biodiesel yield was analyzed based on response surface regression using the second-order polynomial as shown in Equation 1:

$$Y = \beta_0 + \beta_0 X_1 + \beta_2 X_2 + \beta_3 X_3 + \beta_{12} X_1 X_2 + \beta_{13} X_1 X_3 + \beta_{23} X_2 X_3 + \beta_{11} X_1^2 + \beta_{22} X_2^2 + \beta_{33} X_3^2 \quad (1)$$

where Y is the predicted biodiesel yield, β_0 is the intercept value; β_1, β_2 and β_3 are the linear coefficients, β_{12}, β_{13} and β_{23} are the interactive coefficient, β_{11}, β_{22} and β_{33} are the quadratic coefficients and X_1, X_2 and X_3 are the code factors for each independent variable. Design Expert version 12 software trials (Stat-Ease Inc.) of the quadratic unreduced and reduced models were applied to determine the significance of the model.

Transesterification of palm oil and methanol to biodiesel

Palm oil (100 g) was added into a 500-mL single-necked glass reactor and heated to 65°C. The required amount of methanol to give the desired methanol-to-oil molar ratio (3.95:1, 6:1, 9:1, 12:1 or 14.05:1) was added; the prepared catalyst (2.32 wt.%, 3 wt.%, 4 wt.%, 5 wt.% or 5.68 wt.% compared to palm oil) was mixed until it reached the selected temperature, whereupon it was maintained with stirring at 500 rpm for different times (39.55 min, 60 min, 90 min, 120 min or 140.45 min). After transesterification, the reaction mixture was filtrated to remove the catalyst. The biodiesel-containing reaction filtrate was washed several times with distilled water at 60 °C until the pH reached 7 to remove excess methanol and glycerol. Lastly, the obtained biodiesel was kept in a glass bottle containing anhydrous sodium sulfate.

Analysis of biodiesel composition

The ester content, as the mono-, di- and tri-glyceride compositions of the obtained biodiesel, was identified using thin layer chromatography/flame ionization detection (IATROSCAN MK-65 model). Afterward, the optimum

Table 2 Independent factors used for central composite design for transesterification of palm oil and methanol using the 30K-MA catalyst

Factor	Symbol	Coded factor level				
		-2	-1	0	+1	+2
Catalyst loading (wt.%)	X_1	2.32	3	4	5	5.68
Methanol-to-oil molar ratio	X_2	3.95:1	6:1	9:1	12:1	14.05:1
Reaction time (min)	X_3	39.55	60	90	120	140.45

wt.% = weight percentage

conditions of palm oil-biodiesel were characterized using gas chromatography with a Hewlett-Packard 5890 Series II equipped with a FID and a DB-WAX (30 m × 0.25 mm) fused-silica capillary column coated with a 0.1 µm film. Helium (99.99%) as the carrier gas was set at a flow rate of 70 mL/min. Fatty acid (0.2 µL) was injected into the oven (155 °C) with an injector and the detector temperature was 200 °C with a split ratio of 75:1 and 230 °C, respectively. After an isothermal period of 20 min, the temperature was increased to 220 °C at a rate of 2 °C/min and held for 15 min, for a total analysis time of 62 min. The biodiesel composition was identified from the fraction of the area under the peak at different retention times.

Catalyst reusability

To investigate the reuse of the catalyst, after the transesterification reaction, the recovered solid catalyst from the filtration step was washed with hexane solution to eliminate the excess methanol and then dried in an oven at 105 °C overnight. The solid catalyst was used in the same transesterification reaction process to evaluate the reusability of catalyst under optimized conditions (4.53 wt.% catalyst loading, 10.8:1 methanol-to-oil molar ratio and 98.7 min reaction time at 65 °C).

Results and Discussion

Influence of K_2CO_3 loading level on catalytic performance

Fig. 1 shows the relationship between the K_2CO_3 loadings level on the αK-MA catalyst and its catalytic performance for biodiesel production via transesterification of palm oil with methanol. The biodiesel yield over the MA support (with no K_2CO_3) was 8.94%, reflecting the low alkaline content and low basicity (0.84 mmol/g) of MA. As the K_2CO_3 loading level on MA increased, the obtained biodiesel yield increased up to 96.50% for the reaction catalyzed using 30K-MA, since the increasing level of K species and basic strength of the catalyst enhanced the catalytic performance. However, the biodiesel yield was only slightly increased (96.95%) when the K_2CO_3 loading level was further increased from 30 wt.% to 35 wt.%, due to the agglomeration and poor dispersion of the K species on the surface of the catalyst (Zhao et al., 2018). Hence, the 30K-MA catalyst was selected for determination of the optimum parameters of the palm oil and methanol transesterification reaction.

Catalyst characterization

Table 3 lists the basic strength and basicity of all samples. The basic strength was ranked as follows: 35K-MA > 30K-MA > 25K-MA > MA catalyst. The MA exhibited a mildly basic strength (7.2 < H_ <9.8) and the lowest total basicity (0.84 mmol/g), due to having only a slight alkaline content, which was unsuitable for catalyzing the transesterification reaction. However, increasing the K_2CO_3 levels doped on the MA up to 35 wt.% increased the basicity (as expected), which was able to enhance the catalytic activity.

The morphology and surface analysis of each catalyst was determined based on the SEM analysis. Fig. 2 shows representative SEM images of the MA support and 30K-MA catalyst at 1,000× magnification, with cavities evident on the MA surface. After the K_2CO_3 loading, the morphology of the 30K-MA catalyst was changed to a channel structure due to the K compounds covering the surface of the MA.

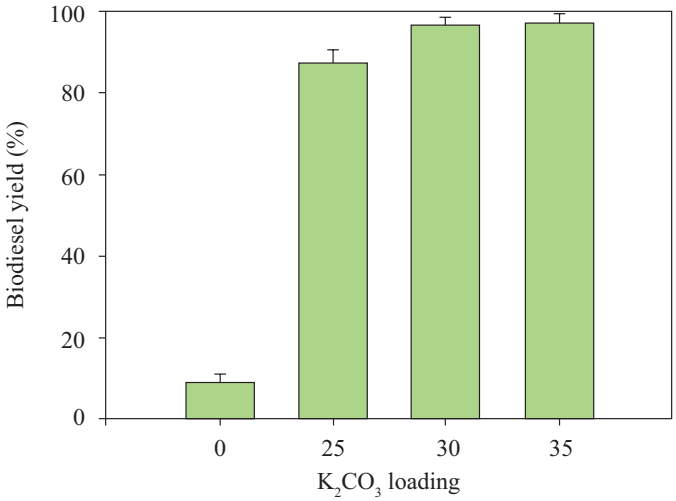

Fig. 1 Effect of K_2CO_3 loading level on biodiesel yield, where reaction conditions were 4 weight percent catalyst loading level, 9:1 methanol-to-palm oil molar ratio, 90 min reaction time and 65 °C reaction temperature.

Table 3 Basic strength and total basicity of prepared mangosteen peel ash (MA) and αK-MA catalysts

Catalyst	Basic strength (H_)[a]	Total basicity (mmol/g)[b]
MA	7.2 < H_ <9.8	0.84
25K-MA	9.8 < H_ <15.0	5.83
30K-MA	9.8 < H_ <15.0	7.83
35K-MA	9.8 < H_ <15.0	7.90

[a] = measured using Hammett indicator method;
[b] = determined using titration method

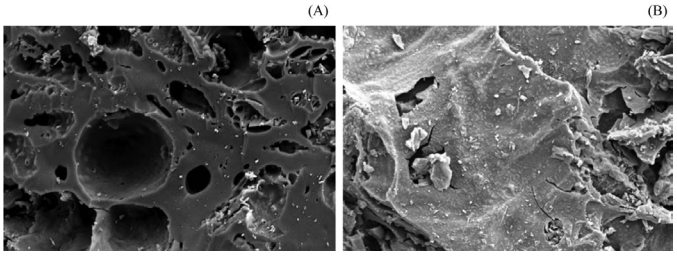

Fig. 2 Representative scanning electron microscopy images (1,000× magnification) of (A) mangosteen peel ash (MA); (B) 30K-MA catalyst

Zhao et al. (2018) reported that the biochar had a surface morphology like air-dried raw moss, which was smooth and wrinkled. After K_2CO_3 activation, the sample had a regular, channeled structure. With the K compounds covering the surface of the biochar, irregular particles were observed on the surface of the biochar sheet, which had a very different appearance from previous samples.

Table 4 presents the elemental composition of the MA support and 30K-MA catalyst as analyzed using EDS. The MA was comprised of mainly carbon (84.82%) as the biomass had high carbon content after calcination and was similar in composition to other waste biomass-activated carbon (González et al., 2017; Gohain et al., 2017; Barros et al., 2020; Tang et al., 2020). The MA had a low potassium content, which contributed to the alkaline content; therefore, this was appropriate as a catalyst support for biodiesel production. In addition, it was notable that for the 30K-MA catalyst, the carbon content decreased, while the potassium content increased, which suggested that the loaded potassium was well scattered over the MA. Zhao et al. (2018) also reported that the activated biochar consisted mainly of carbon with only small amounts of metal oxides.

The FTIR spectra of the MA and 30K-MA catalysts are represented in Fig. 3. The adsorption band at wave numbers 658 cm^{-1} and 1630 cm^{-1} was attributed to the O–H stretching vibrations of atmospheric water. Similarly, the same peaks have been reported by Betiku et al. (2016). The peak band at 878 cm^{-1} represented the phase of the CO_3^{2-} species, which was due to the CO_2 in the air adsorbed from the surrounding environment. After the formation of the 30K-MA catalyst, the range of the observed absorption peaks shifted compared to the MA catalyst, which may have been due to the K_2CO_3 in the catalyst structure. The FTIR spectrum of the 30K-MA catalyst had a strong adsorption band around 1399 cm^{-1}, which was attributed to the phase of K_2CO_3 loaded on the MA (Zhao et al., 2018). This again confirmed the success of adding K_2CO_3 active sites onto the MA support for application in the transesterification reaction for biodiesel synthesis.

Fig. 4 shows the XRD patterns of the prepared MA and the 30K-MA catalyst over the 2θ range of 10–90°. The MA support without K_2CO_3 impregnation had two broad peaks between 2θ values of 11.07°–30.72° and 34.34°–50.07°, which corresponded to the non-graphitic carbon (C), since the MA had a high C content of about 84% after calcination, as supported by the EDS analysis (Zhao et al., 2018; Tang et al., 2020). The XRD spectrum of the 30K-MA catalyst contained peaks at 2θ values of 25.78°, 31.65°, 41.62° and 44.96° that corresponded with the K_2O and K_2CO_3 phases (Tang et al., 2020). The K_2O phase was formed during the calcination step and led to the strong basic sites.

Table 4 Representative energy dispersive X-ray spectroscopy results of the surface of mangosteen peel ash (MA) and 30K-MA catalyst

Catalyst	Surface area (m^2/g)[a]	Element content[b] (weight percentage)		
		C	O	K
MA	39.07	84.82	9.97	5.21
30K-MA	14.11	58.93	20.82	20.25

[a] = determined using N_2 adsorption-desorption;
[b] = measured using energy dispersive X-ray spectroscopy

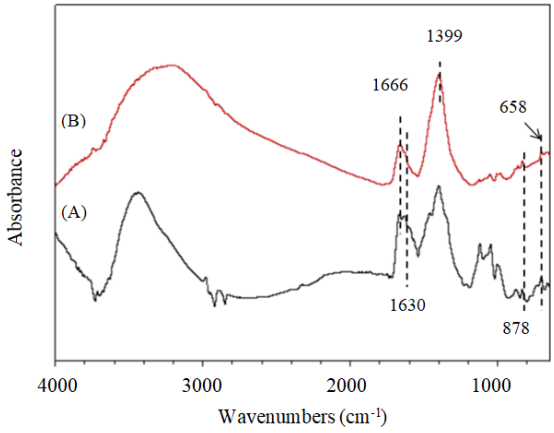

Fig. 3 Representative Fourier-transform infrared spectrum of: (A) mangosteen peel ash (MA); (B) 30K-MA catalyst

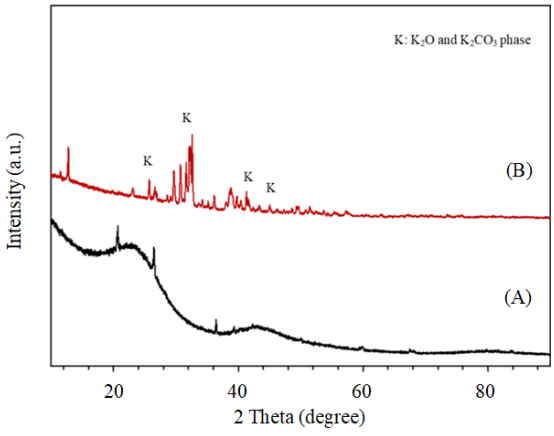

Fig. 4 Representative X-ray diffraction patterns of: (A) mangosteen peel ash (MA); (B) 30K-MA catalyst, where K = K_2O and K_2CO_3 phase

Table 4 shows the BET specific surface area of the MA support and 30K-MA catalyst. The specific surface area of MA was relatively high (39.07 m^2/g) but substantially decreased by approximately 60% in the 30K-MA catalyst (14.11 m^2/g). Decreasing the surface area was essential to provide active sites occupied by the K groups on the MA support that were required to enhance the catalytic performance in the transesterification reaction.

Fig. 5 shows the existence of different elements on the catalyst surface, based on the XPS analysis. For this purpose, a wide scan mode of the prepared catalyst was performed in the range 0–1200 eV to determine the C, oxygen (O), and potassium (K) element contents. For the MA (Fig. 5A), a band was noticed at BEs of 529 eV, 291 eV, and 291 eV, which were attributed to O 1s (15.83%), C 1s (67.23%) and K 2p (16.94%), respectively. High resolution scans of the MA (Fig. 5B) were performed to measure the K 2p element at 293.40 eV (49.38%) and 295.95 eV (50.62%). For the 30K-MA catalyst (Figs. 5C–5D), the BE values were in the range 292.85–295.57 eV that revealed the K 2p groups corresponding to the K–O functional group had successfully anchored on the surface of the prepared catalyst to act as active sites for the transesterification reaction (biodiesel production).

Optimization of process parameters using response surface methodology

The results from the analysis of variance and regression model are listed in Table 5. The six-replicate reactions run at the central point (reaction conditions: 4 wt.% catalyst loading, 9:1 methanol-to-oil molar ratio and 90 min reaction time at 65 °C) produced an average biodiesel yield of 96.6 ± 0.2%. The analysis of variance of the unreduced model for biodiesel production was validated (Table 6), with the final quadratic regression equation of the unreduced model shown in Equation 2:

$$\begin{aligned}\text{Biodiesel yield} = {} & 0.083190 - 1.45725X_1 + 19.90215X_2 - 0.038338X_3 - \\ & 0.066250X_1X_2 + 0.005875X_1X_3 + 0.002875X_2X_3 + \\ & 0.203999X_1^2 - 0.969444X_2^2 - 0.000021X_3^2 \end{aligned} \quad (2)$$

where, X_1, X_2 and X_3 are the catalyst loading (as weight percentage), methanol-to-oil molar ratio and reaction time (in minutes), respectively.

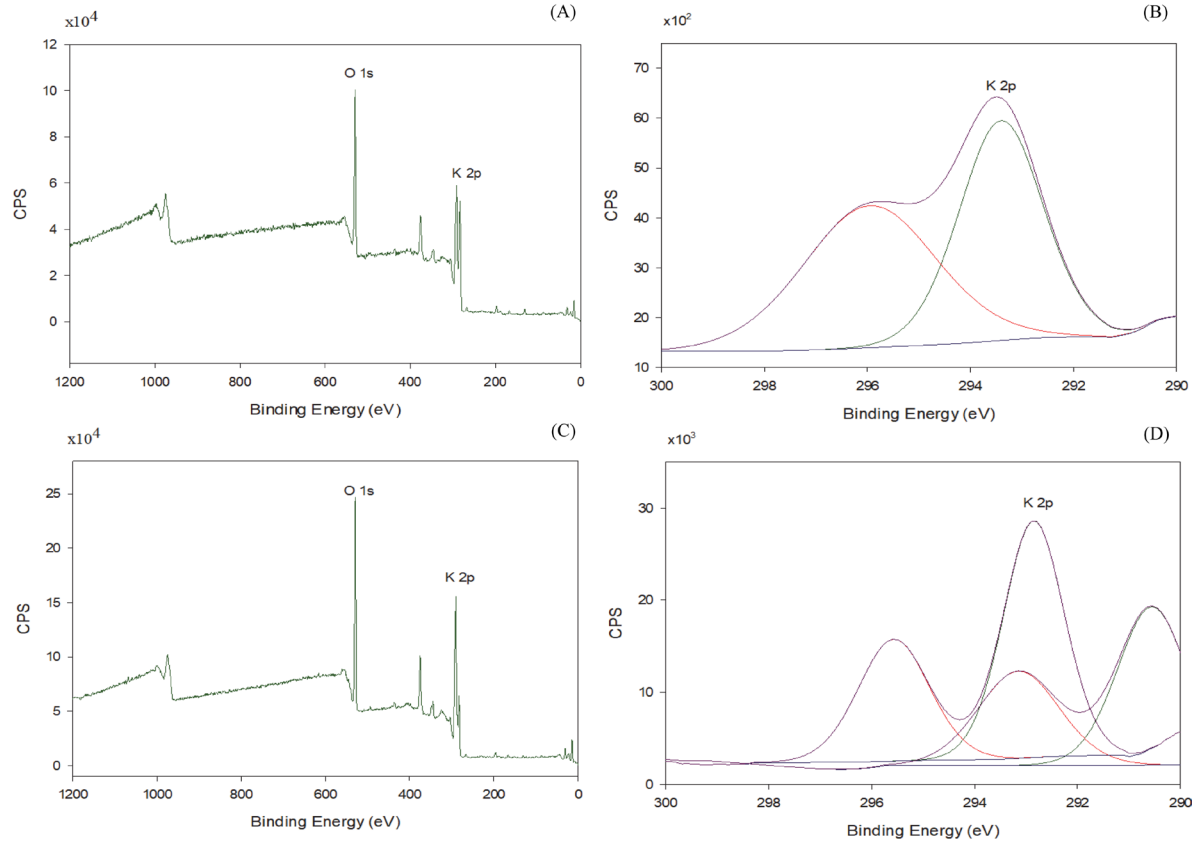

Fig. 5 Representative X-ray photoelectron spectra of: (A) mangosteen peel ash (MA, wide scan mode); (B) MA (narrow scan mode); (C) 30K-MA (wide scan mode); (D) 30K-MA (narrow scan mode) catalyst

Table 5 Actual and predicted values for response surface analysis

Run	Catalyst loading (wt.%) (X_1)	Methanol-to-oil molar ratio (X_2)	Reaction time (min) (X_3)	Observed biodiesel yield (%)	Predicted biodiesel yield (%)	Residual
1	4	9:1	140.45	95.50	96.87	-1.37
2	3	12:1	120	96.30	95.74	0.56
3	4	3.95:1	90	58.30	59.53	-1.23
4	4	14.05:1	90	84.13	84.21	-0.08
5	5.68	9:1	90	96.73	97.31	-0.58
6	2.32	9:1	90	96.21	96.95	-0.74
7	5	12:1	60	94.50	94.61	-0.11
8	5	12:1	120	96.40	95.91	0.49
9	4	9:1	39.55	96.18	96.13	0.05
10	5	6:1	60	81.22	80.84	0.38
11	5	6:1	120	82.09	81.12	0.97
12	3	6:1	120	81.19	80.15	1.04
13	3	12:1	60	95.10	95.14	-0.04
14	3	6:1	60	81.03	80.59	0.44
15	4	9:1	90	96.34	96.55	-0.21
16	4	9:1	90	96.50	96.55	-0.05
17	4	9:1	90	96.80	96.55	0.25
18	4	9:1	90	96.35	96.55	-0.2
19	4	9:1	90	96.75	96.55	0.2
20	4	9:1	90	96.80	96.55	0.25

wt.% = weight percentage

Table 6 Analysis of variance results of quadratic unreduced model for biodiesel production using calcined 30K-MA as heterogeneous catalyst

Source	Sum of Squares	df	Mean Square	F-value	*p*-Value
Model	1859.25	9	206.58	277.08	< 0.0001
X_1	0.1571	1	0.1571	0.2107	0.6561
X_2	735.32	1	735.32	986.27	< 0.0001
X_3	0.6530	1	0.6530	0.8759	0.3714
X_1X_2	0.3160	1	0.3160	0.4239	0.5297
X_1X_3	0.2485	1	0.2485	0.3333	0.5765
X_2X_3	0.5356	1	0.5356	0.7184	0.4165
X_1^2	0.5997	1	0.5997	0.8044	0.3909
X_2^2	1097.07	1	1097.07	1471.46	< 0.0001
X_3^2	0.0051	1	0.0051	0.0068	0.9360
Residual	7.46	10	0.7456		
Lack of fit	7.21	5	1.44	29.81	0.0010
Pure error	0.240	5	0.0484		
Cor total	1866.70	19			

R^2 = 0.9960, Adj R^2 = 0.9924

df = degrees of freedom; R^2 = coefficient of determination; Adj = adjusted; X_1 = catalyst loading; X_2 = methanol-to-oil molar ratio; X_3 = reaction time

At the 95% confidence level, the results of the quadratic unreduced model revealed that the response equation for biodiesel was appropriate. The results showed that the methanol-to-oil molar ratio had the major effect on biodiesel production (highest F value and *p* value < 0.0001). However, there were no significant effects on the biodiesel yield for the catalyst loading, reaction time, interaction between the catalyst loading level and the methanol-to-oil molar ratio, interaction between the catalyst loading and reaction time, and the interaction between the methanol-to-oil molar ratio and the reaction time. The F value of the lack of fit of the quadratic unreduced model was 29.81, which indicated that the lack of fit was not significant. The polynomial model, based on the values of the coefficient of determination (R^2) = 0.9960 and the adjusted coefficient of determination (Adj R^2) = 0.9924 showed a high correlation between the actual and predicted values.

The analysis of variance testing of the quadratic reduced model to eliminate the not significant parameters is described in Table 7. The biodiesel yield from the reduced quadratic model was estimated using Equation 3:

$$\text{Biodiesel yield} = -3.99859 + 19.92937X_2 - 0.971303X_2^2 \quad (3)$$

Table 7 Analysis of variance results of quadratic reduced model for biodiesel production using calcined 30K-MA as heterogeneous catalyst

Source	Sum of Squares	df	Mean Square	F-value	*p*-Value
Model	1856.72	2	928.36	1580.15	< 0.0001
X_2	735.32	1	735.32	1251.59	< 0.0001
X_2^2	1121.39	1	1121.39	1908.71	< 0.0001
Residual	9.99	17	0.5875		
Lack of fit	9.75	12	0.8121	16.78	0.0029
Pure error	0.2420	5	0.0484		
Cor total	1866.70	19			
$R^2 = 0.9946$, Adj $R^2 = 0.9940$					

Df = degrees of freedom; R^2 = coefficient of determination; Adj = adjusted; X_1 = catalyst loading; X_2 = methanol-to-oil molar ratio; X_3 = reaction time.

The quadratic regression model F value was 1580.15 and the *p* value was less than 0.0001, indicating that the quadratic regression model was significant. The most significant parameter effect in the quadratic reduced model was the methanol-to-oil molar ratio, with $p < 0.0001$. The R^2 and Adj R^2 values were 0.9946 and 0.9940, respectively, showing a high correction between the predicted and observed biodiesel values.

Fig. 6 shows the correlation between the actual and predicted biodiesel yields for each of the various effects and shows that the error distribution was close to zero, since all the points were close to the line of perfect fit.

Influence of studied parameters on biodiesel yield

The Design Expert version 12 trials were used to predict the biodiesel yield in the transesterification of palm oil with methanol for the different parameters of methanol-to-oil molar ratio, reaction time and catalyst loading level using the 30K-MA catalyst (since it had a higher catalytic performance than the others).

Interactive effect between catalyst loading level and methanol-to-oil molar ratio

Fig. 7 shows the interaction effect of the catalyst loading level and the methanol-to-oil molar ratio on the biodiesel yield at a fixed 65 °C reaction temperature and 90 min reaction time. The catalyst amount was in the range 2.32–5.68 wt.% of the starting palm oil amount. From the three-dimensional (3D) plot, the combination effect of the catalyst loading level and methanol-to-palm oil molar ratio was not significant. As can be seen in Table 6, the effect of the catalyst loading level was not significant regarding biodiesel production.

Increasing the catalyst loading from 3 wt.% to 5 wt.% with a methanol-to-palm oil molar ratio of 6:1 and 60 min of reaction time slightly increased the biodiesel yield from 80.6% to 80.8%, while a catalyst loading of 4.53 wt.% produced the optimum biodiesel yield of 98.0% at a methanol-to-palm oil ratio of 10.8:1, due to the high density of basic sites of catalysts (Pavlović et al., 2020; Wadood et al., 2020).

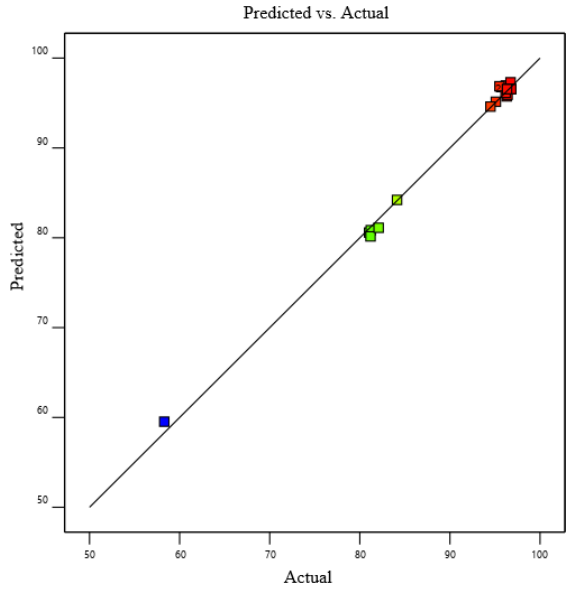

Fig. 6 Comparison between actual and predicted values using response surface methodology

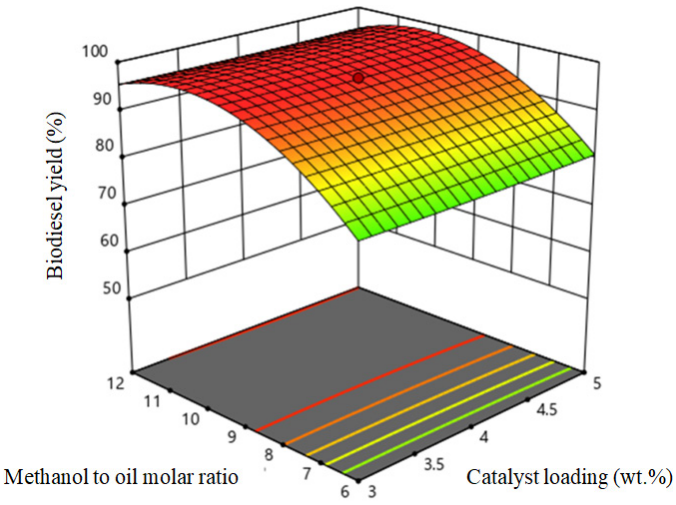

Fig. 7 Surface response plots showing predicted values of biodiesel yield with interaction effect of catalyst loading level and methanol-to-oil molar ratio

Increasing the methanol-to-palm oil molar ratio from 6:1 to 12:1, under the operating parameters of 3 wt.% catalyst and 60 min reaction time, significantly enhanced the biodiesel yield from 80.6% to 95.1%. This was mainly due to the abundance of reactants that resulted in a high probability of collision between the reactant and solid catalyst (Yahya et al., 2020). The highest biodiesel yield (98.0%) was produced at a methanol-to-palm oil molar ratio of 10.8:1. When the methanol-to-oil molar ratio was lower than 3:1, the biodiesel yield decreased due to the limiting number of reactant molecules and so a reduced level of methoxy species were formed (Hoseini et al., 2019; Mujtaba et al., 2020). However, a methanol-to-oil molar ratio higher than 10.8:1 significantly decreased the biodiesel yield, since excessive methanol led to an emulsified solution mixture and blocked the K^+ species on the solid catalyst during the transesterification process. From the experimental results, the methanol-to-oil molar ratio had a more significant effect on the biodiesel production than the catalyst loading effect.

Interactive effect between reaction time and methanol-to-oil molar ratio

Fig. 8 shows the interaction effect of the reaction time and methanol-to-oil molar ratio on the biodiesel yield for a reaction temperature at 65 °C and a 4 wt.% catalyst loading level. From the 3D response surface plot, the combined effect between the reaction time and the methanol-to-palm oil molar ratio was not significant. Increasing the reaction time from 60 min to 120 min under a catalyst loading of 5 wt.% and a 6:1 methanol-to-palm oil molar ratio slightly increased the biodiesel yield from 80.8% to 81.1%. The increased reaction time resulted in an increased amount of electrophile sites through transesterification and favored the formation of fatty acid methyl esters (Fatimah et al., 2019; Behera et al., 2020). This observation was substantiated by Mutalib et al. (2020), Samuel et al. (2020) and Samuel et al. (2021a, b).

The optimum operating reaction parameters were predicted to be a catalyst loading of 4.53 wt.%, methanol-to-palm oil molar ratio of 10.8:1 and a reaction time of 98.7 min, producing a biodiesel yield of 98.0%, as shown in Fig. 9.

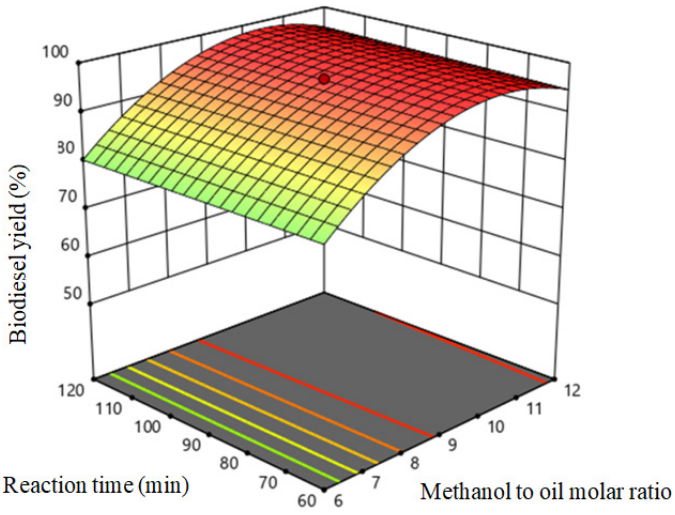

Fig. 8 Surface response plots showing predicted values of biodiesel yield, interaction effect of reaction time and methanol-to-oil molar ratio

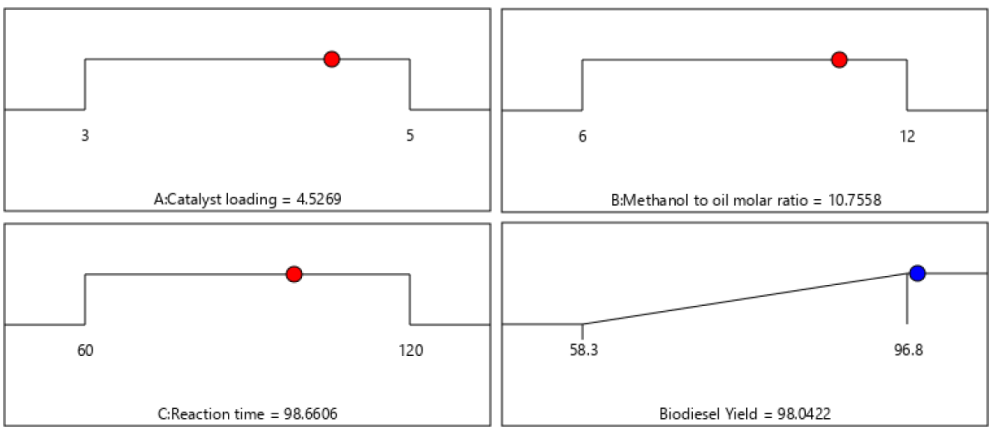

Fig. 9 Optimal reaction conditions for transesterification of palm oil with methanol over 30K-MA catalyst

Reusability of 30K-MA catalyst

Many solid catalysts derived from waste biomass for use in biodiesel production through transesterification have been shown to be reusable in multiple reaction cycles; however, the reusability properties of the 30K-MA catalyst regarding biodiesel yield are unknown. Thus, the 30K-MA catalyst was tested using the initial reaction conditions of 4.53 wt.% catalyst loading, 10.8:1 methanol-to-palm oil molar ratio, 98.7 min reaction time and a reaction temperature of 65 °C. After each transesterification cycle, the reaction mixture was filtered and the recovered catalyst was washed with hexane several times and dried in an oven overnight before reuse in a new transesterification cycle. Fig. 10 shows the reusability of the 30K-MA catalyst, where the obtained biodiesel yield significantly decreased over four consecutives runs from 97.9% to 86.3%, 76.6% and 65.1%, respectively. The decreased biodiesel yield likely reflected the catalyst deactivation or leaching of K metal from the catalyst into the liquid phase, which increased product contamination from the catalyst (Mutalib et al., 2020; Jitjamnong et al., 2021). Mares et al. (2021) studied the reuse of the catalyst derived from the acai seed ash and observed that in the fourth reaction run, the ester content of the biodiesel was 36.2%. They reported that the significant decrease in biodiesel yield may have been due to the filling of pores and the poisoning of the catalyst surface by triglycerides and glycerol, thereby reducing the number of active sites, which in turn reduced the conversion of triglycerides into biodiesel. Aleman-Ramirez et al. (2022) noted that the catalysts could be reused after pretreatment prior to successive reaction runs using recalcination to reactivate the catalyst by decomposing any trace organic material that could cover up the catalyst surface.

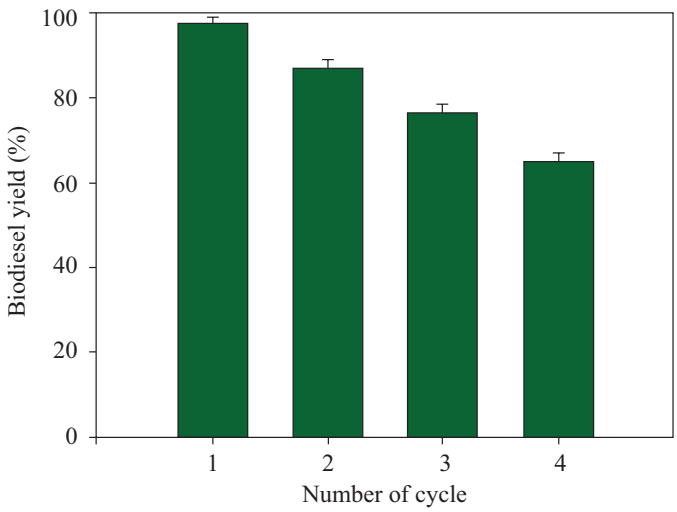

Fig. 10 Reusability of 30K-MA catalyst

Composition and physicochemical properties of biodiesel using 30K-MA catalyst

The composition of the obtained biodiesel was evaluated using gas chromatography-flame ionization detection (GC-FID) to confirm the biodiesel profile, as shown in Table 8. The 30K-MA catalyst was used under the optimum transesterification conditions (4.53 wt.% catalyst loading, 10.8:1 methanol-to-oil molar ratio and 98.7 min reaction time at 65 °C). The biodiesel contained 45.7% mono-saturated fats, followed by 41.8% saturated fats, 10.2% di-unsaturated fats and 0.3% tri-unsaturated fats content, respectively. The physicochemical properties of the biodiesel produced in the current study (ester content, density at 15 °C, kinematic viscosity at 40 °C and carbon residue) were compared with the standard specifications of ASTM D 6751 and the EN 14214 standards and are presented in Table 9. The content of fatty acid methyl esters was 97.89%, which is within the range specified in EN 14214. The density and the kinematic viscosity of the obtained biodiesel were 876 kg/m^3 and 4.7 mm^2/s, respectively. The kinematic viscosity can be used not only as an indicator of contaminants in biodiesel, but also as a control parameter of the transesterification process (Ellis et al., 2008; Černoch et al., 2010). Biodiesel derived from palm oil via transesterification over a biochar-based catalyst from waste pomelo peel had a density of 884 kg/m^3 and a kinematic viscosity of 3.68 mm^2/s (Zhao et al., 2018). The carbon residue of biodiesel in the current study was less than 0.01%, which is within the range specified in ASTM D 6751 standards.

Table 8 Composition of biodiesel synthesized from palm oil and methanol using 30K-MA catalyst

Chemical	Structure of carbon	Composition (%)[a]
Saturated		
Palmitic	C16:0	37.12
Heptadecanoic	C17:0	0.12
Stearic	C18:0	3.95
Arachidic	C20:0	0.48
Docosanoic	C24:0	0.11
Mono-unsaturated		
cis-Oleic	*cis*-C18:1	45.55
trans-Eicosenoic	*trans*-C20:1	0.16
Di-unsaturated		
Linoleic	C18:2	10.15
Tri-unsaturated		
Linolenic	C18.3	0.25
Total ester content		97.89

[a] = measured using gas chromatography-flame ionization detection (reaction conditions: 4.53 wt.% catalyst loading level, 10.76:1 methanol-to-palm oil molar ratio, 98.66 min reaction time and 65 °C reaction temperature).

Table 9 Physicochemical properties of biodiesel using 30K-MA catalyst

Properties	ASTM D 6751 standards	EN 14214 standards	Current study
Ester content	-	96.5% min	97.89%
Density at 15 °C (kg/m^3)	-	860–900	876
Kinematic viscosity at 40 °C (mm^2/s)	1.9–6.0	3.5–5.0	4.7
Carbon residue (wt.%)	0.050	-	< 0.01

wt.% = weight percentage

Comparison of various biomass-derived heterogeneous catalysts for biodiesel production

The results of the current study and other works on biodiesel synthesis via transesterification reaction are provided in Table 10 and show that the biodiesel yield from the current experiment was comparatively high at 97.9%, compared to other biodiesel yields (Lathiya et al., 2018; Fatimah et al., 2019; Mendonça et al., 2019b; Foroutan et al., 2022; Daimary et al., 2022). The 30K-MA catalyst showed excellent potential and activity compared to other catalysts, suggesting that the 30K-MA catalyst has high potential.

Conclusion

MA was synthesized as a potential renewable support for a K_2O-based alkali heterogeneous catalyst for biodiesel production based on transesterification. Biodiesel production was optimized using RSM with a CCD model to study the effects of the catalyst loading, methanol-to-palm oil molar ratio and reaction time at a constant 65 °C reaction temperature. The optimal biodiesel yield of 97.9% was obtained at a 30K-MA loading level of 4.53 wt.%, a methanol-to-palm oil molar ratio of 10.8:1, a reaction time of 98.7 min and reaction temperature of 65 °C. The 30K-MA catalyst was relatively stable (biodiesel yield of > 65%) for four successive transesterification cycles. The characterization study indicated that the alkaline properties and morphology of the 30K-MA catalyst supported its potential for biodiesel production based on a transesterification reaction.

Conflict of Interest

The authors declare that there are no conflicts of interest.

Acknowledgements

Financial support was provided by the Rajamangala University of Technology Srivijaya, Songkhla, Thailand.

Table 10 Comparison of synthesized catalyst with other biomass-based heterogeneous base catalysts

Catalyst	Reaction conditions				Biodiesel yield (%)	Reference
	M:O molar ratio	Cat. loading (wt.%)	Temp. (°C)	Time (min)		
Walnut shell ash/ZnO/K_2CO_3	18:1	4.0	65	240	97.3	Foroutan et al. (2022)
Bamboo leaf ash/ZrO_2	15:1	12.0	50	30	92.8	Fatimah et al. (2019)
Potato peel biochar	9:1	3.00	60	120	97.5	Daimary et al. (2022)
Tucumã peels	15:1	1.00	80	240	97.3	Mendonça et al. (2019b)
Waste orange peel	19.95:1	5.00	65	274	91.7	Lathiya et al. (2018)
30K–MA	10.8:1	4.53	65.0	98.7	97.9	This study

M:O = methanol to oil, Cat. = catalyst, Temp. = temperature

References

Abdullah, S.H.Y.S., Hanapi, N.H.M., Azid, A., Umar, R., Juahir, H., Khatoon, H., Endut, A. 2017. A review of biomass-derived heterogeneous catalyst for a sustainable biodiesel production. Renew. Sust. Energ. Rev. 70: 1040–1051. doi.org/10.1016/j.rser.2016.12.008

Abu-Jrai, A.M., Jamil, F., Al-Muhtaseb, A.H., Baawain, M., Al-Haj, L., Al-Hinai, M., Al-Abri, M., Rafiq, S. 2017. Valorization of waste Date pits biomass for biodiesel production in presence of green carbon catalyst. Energ. Convers. Manage. 135: 236–243. doi.org/10.1016/j.enconman.2016.12.083

Adepoju, T.F., Rasheed, B., Olatunji, O.M., Ibeh, M.A., Ademiluyi, F.T., Olatunbosun, B.E. 2018. Modeling and optimization of lucky nut biodiesel production from lucky nut seed by pearl spar catalysed transesterification. Heliyon 4: e00798. doi.org/10.1016/j.heliyon.2018.e00798

Ahmad, M.A., Alrozi, R. 2010. Optimization of preparation conditions for mangosteen peel-based activated carbons for the removal of Remazol Brilliant Blue R using response surface methodology. Chem. Eng. J. 165: 883–890. doi.org/10.1016/j.cej.2010.10.049

Aizat, W.M., Ahmad-Hashim, F.H., Jaafar, S.N.S. 2019. Valorization of mangosteen, "The Queen of Fruits," and new advances in postharvest and in food and engineering applications: A review. J. Adv. Res. 20: 61–70. doi.org/10.1016/j.jare.2019.05.005

Aleman-Ramirez, J.L., Okoye, P.U., Torres-Arellano, S., Paraguay-Delgado, F., Mejía-López, M., Moreira, J., Sebastian, P.J. 2022. Development of reusable composite eggshell-moringa leaf catalyst for biodiesel production. Fuel 324: 124601. doi.org/10.1016/j.fuel.2022.124601

Arumugam, A., Sankaranarayanan, P. 2020. Biodiesel production and parameter optimization: An approach to utilize residual ash from sugarcane leaf, a novel heterogeneous catalyst, from *Calophyllum inophyllum* oil. Renew. Energ. 153: 1272–1282. doi.org/10.1016/j.renene.2020.02.101

Balajii, M., Niju, S. 2019. A novel biobased heterogeneous catalyst derived from *Musa acuminata* peduncle for biodiesel production – Process optimization using central composite design. Energ. Convers. Manage. 189: 118–131. doi.org/10.1016/j.enconman.2019.03.085

Balajii, M., Niju, S. 2020. Banana peduncle – A green and renewable heterogeneous base catalyst for biodiesel production from *Ceiba pentandra* oil. Renew. Energ. 146: 2255–2269.

Barros, S.S., Pessoa Junior, W.A.G., Sá, I.S.C., et al. 2020. Pineapple (*Ananas comosus*) leaves ash as a solid base catalyst for biodiesel synthesis. Bioresour. Technol. 312: 123569. doi.org/10.1016/j.biortech.2020.123569

Bastos, R.R.C., Corrêa, A.P.L., Luz, P.T.S., Filho, G.N.R., Zamian, J.R., Conceição, L.R.V. 2020. Optimization of biodiesel production using sulfonated carbon-based catalyst from an amazon agro-industrial waste. Energ. Convers. Manage. 205: 112457. doi.org/10.1016/j.enconman.2019.112457

Behera, B., Selvam, M.S., Dey, B., Balasubramanian, P. 2020. Algal biodiesel production with engineered biochar as a heterogeneous solid acid catalyst. Bioresour. Technol. 310: 123392. doi.org/10.1016/j.biortech.2020.123392

Betiku, E., Akintunde, A.M., Ojumu, T.V. 2016. Banana peels as a biobase catalyst for fatty acid methyl esters production using Napoleon's plume (*Bauhinia monandra*) seed oil: A process parameters optimization study. Energy 103: 797–806. doi.org/10.1016/j.energy.2016.02.138

Cao, X., Sun, S., Sun, R. 2017. Application of biochar-based catalysts in biomass upgrading: A review. RSC Adv. 7: 48793–48805. doi.org/10.1039/C7RA09307A

Černoch, M., Hájek, M., Skopal, F. 2010. Relationships among flash point, carbon residue, viscosity and some impurities in biodiesel after ethanolysis of rapeseed oil. Bioresour. Technol. 101: 7397–7401. doi.org/10.1016/j.biortech.2010.05.003

Changmai, B., Sudarsanam, P., Rokhum, L. 2020. Biodiesel production using a renewable mesoporous solid catalyst. Ind. Crop. Prod. 145: 111911. doi.org/10.1016/j.indcrop.2019.111911

Chingakham, C., David, A., Sajith, V. 2019. Fe_3O_4 nanoparticles impregnated eggshell as a novel catalyst for enhanced biodiesel production. Chinese. J. Chem. Eng. 27: 2835–2843. doi.org/10.1016/j.cjche.2019.02.022

Chua, S.Y., Periasamy, L., Goh, C.M.H., et al. 2020. Biodiesel synthesis using natural solid catalyst derived from biomass waste – A review. J. Ind. Eng. Chem. 81: 41–60. doi.org/10.1016/j.jiec.2019.09.022

Cong, W.J., Wang, Y.T., Li, H., et al. 2020. Direct production of biodiesel from waste oils with a strong solid base from alkalized industrial clay ash. Appl. Energ. 246: 114735. doi.org/10.1016/j.apenergy.2020.114735

Daimary, N., Eldiehy, K.S.H., Eldiehy, P., Deka, D., Bora, U., Kakati, B.K. 2022. Potato peels as a sustainable source for biochar, bio-oil and a green heterogeneous catalyst for biodiesel production. J. Environ. Chem. Eng. 10: 107108. doi.org/10.1016/j.jece.2021.107108

Dubey, K.K.D., Jeyaseelan, C., Upadhyaya, K.C., Chimote, V., Veluchamy, R., Kumar, A. 2020. Biodiesel production from *Hiptage benghalensis* seed oil. Ind. Crop. Prod. 144: 112027. doi.org/10.1016/j.indcrop.2019.112027

Ellis, N., Guan, F., Chen, T., Poon, C. 2008. Monitoring biodiesel production (transesterification) using *in situ* viscometer. Chem. Eng. J. 138: 200–206. doi.org/10.1016/j.cej.2007.06.034

Fatimah, I., Rubiyanto, D., Taushiyah, A., Najah, F.B., Azmi, U., Sim, Y.L. 2019. Use of ZrO_2 supported on bamboo leaf ash as a heterogeneous catalyst in microwave-assisted biodiesel conversion. Sustain. Chem. Pharm. 12: 100129. doi.org/10.1016/j.scp.2019.100129

Foo, K.Y., Hameed, B.H. 2012. Factors affecting the carbon yield and adsorption capability of the mangosteen peel activated carbon prepared by microwave assisted K_2CO_3 activation. Chem. Eng. J. 180: 66–74. doi.org/10.1016/j.cej.2011.11.002

Foroutan, R., Peighambardoust, S.J., Mohammadi, R., Peighambardoust, S.H., Ramavandi, B. 2022. Application of walnut shell ash/ZnO/K_2CO_3 as a new composite catalyst for biodiesel generation from *Moringa oleifera* oil. Fuel 311: 122624. doi.org/10.1016/j.fuel.2021.122624

Gohain, M., Devi, A., Deka, D. 2017. *Musa balbisiana* Colla peel as highly effective renewable heterogeneous base catalyst for biodiesel production. Ind Crop Prod. 109: 8–18. doi.org/10.1016/j.indcrop.2017.08.006

González, M.E., Cea, M., Reyes, D., Romero-Hermoso, L., Hidalgo, P., Meier, S., Benito, N., Navia, R. 2017. Functionalization of biochar derived from lignocellulosic biomass using microwave technology for catalytic application in biodiesel production. Energ. Convers. Manage. 137: 165–173. doi.org/10.1016/j.enconman.2017.01.063

Hoseini, S.S., Najafi, G., Sadeghi, A., 2019. Chemical characterization of oil and biodiesel from Common Purslane (*Portulaca*) seed as novel weed plant feedstock. Ind. Crop. Prod. 140: 111582. doi.org/10.1016/j.indcrop.2019.111582

Jitjamnong, J., Luengnaruemitchai, A., Samanwonga, N., Chuaykarn, N. 2019. Biodiesel production from canola oil and methanol using Ba impregnated calcium oxide with microwave irradiation-assistance. Chiang Mai J. Sci. 46: 987–1000.

Jitjamnong, J., Thunyaratchatanon, C., Luengnaruemitchai, A., Kongrit, N., Kasetsomboon, N., Chuaykarn, N., Khantikulanon, N. 2020a. Effect of calcination temperature of *Musa sapientum* Linn peels as a novel biobased heterogeneous catalyst for soybean oil-derived fatty acid methyl ester formation. Chiang Mai J. Sci. 47: 484–498.

Jitjamnong, J., Thunyaratchatanon, C., Luengnaruemitchai, A., Kongrit, N., Kasetsomboon, N., Sopajarn, A., Chuaykarn, N., Khantikulanon, N. 2020b. Response surface optimization of biodiesel synthesis over a novel biochar-based heterogeneous catalyst from cultivated (*Musa sapientum*) banana peels. Biomass. Conv. Bioref. 11: 2795–2811. doi.org/10.1007/s13399-020-00655-8

Lathiya, D., Bhatt, D.V., Maheria, K.C. 2018. Synthesis of sulfonated carbon catalyst from waste orange peel for cost effective biodiesel production. Bioresour. Technol. Rep. 2: 69–76. doi.org/10.1016/j.biteb.2018.04.007

Li, Y., Wang, X., Cao, M. 2018. Three-dimensional porous carbon frameworks derived from mangosteen peel waste as promising materials for CO_2 capture and supercapacitors. J. CO2 Util. 27: 204–216. doi.org/10.1016/j.jcou.2018.07.019

Mendonça, I.M., Machado, F.L., Silva, C.C., Junior, S.D., Takeno, M.L., Maia, P.J.S., Manzato, L., Freitas, F.A. 2019a. Application of calcined waste cupuaçu (*Theobroma grandiflorum*) seeds as a low-cost solid catalyst in soybean oil ethanolysis: Statistical optimization. Energ. Convers. Manage. 200: 112095. doi.org/10.1016/j.enconman.2019.112095

Mendonça, I.M., Paes, O.A.R.L., Maia, P.J.S., Souza. M.P., Almeida, R.A., Silva, C.C., Duvoisin, S.Jr., Freitas, F.A. 2019b. New heterogeneous catalyst for biodiesel production from waste tucumã peels (*Astrocaryum aculeatum* Meyer): Parameters optimization study. Renew. Energ. 130: 103–110. doi.org/10.1016/j.renene.2018.06.059

Mujtaba, M.A., Masjuki, H.H., Kalam, M.A., et al. 2020. Ultrasound-assisted process optimization and tribological characteristics of biodiesel from palm-sesame oil via response surface methodology and extreme learning machine - Cuckoo search. Renew. Energ. 158: 202–214. doi.org/10.1016/j.renene.2020.05.158

Nguyen, H.C., Nguyen, M.L., Wang, F.M., Juan, H.Y., Su, C.H. 2020. Biodiesel production by direct transesterification of wet spent coffee grounds using switchable solvent as a catalyst and solvent. Bioresour. Technol. 296: 122334. doi.org/10.1016/j.biortech.2019.122334

Mares E.K.L., Gonçalves M.A., Luz, P.T.S., Filho, G.N.R., Zamian, J.R., Conceição, L.R.V. 2021. Acai seed ash as a novel basic heterogeneous catalyst for biodiesel synthesis: Optimization of the biodiesel production process. Fuel 299: 120887. doi.org/10.1016/j.fuel.2021.120887

Mutalib, A.A.A., Ibrahim, M.L., Matmin, J., et al. 2020. SiO_2-rich sugar cane bagasse ash catalyst for transesterification of palm oil. Bioenerg. Res. 13: 986–997. doi.org/10.1007/s12155-020-10119-6

Nasrullah, A., Saad, B., Bhat, A.H., Khan, A.S., Danish, M., Hasnain Isa, M., Naeem, A. 2019. Mangosteen peel waste as a sustainable precursor for high surface area mesoporous activated carbon: Characterization and application for methylene blue removal. J. Clean. Prod. 211: 1190–1200. doi.org/10.1016/j.jclepro.2018.11.094

Pandit, P.R., Fulekar, M.H. 2019. Biodiesel production from microalgal biomass using CaO catalyst synthesized from natural waste material. Renew. Energ. 136: 837–845. doi.org/10.1016/j.renene.2019.01.047

Pavlović, S.M., Marinković, D.M., Kostić, M.D., Janković-Častvan, I.M., Mojović, L.V., Stanković, M.V., Veljković, V.B. 2020. A CaO/zeolite-based catalyst obtained from waste chicken eggshell and coal fly ash for biodiesel production. Fuel 267: 117171. doi.org/10.1016/j.fuel.2020.117171

Samuel, O.D., Okwu, M.O., Oyejide, O.J., Taghinezhad, E., Afzal, A., Kaveh, M. 2020. Optimizing biodiesel production from abundant waste oils through empirical method and grey wolf optimizer. Fuel 281: 118701. doi.org/10.1016/j.fuel.2020.118701

Samuel, O.D., Waheed, M.A., Garavand, A.T., Verma, T.N., Dairo, O.U., Bolaji, B.O., Afzal, A. 2021. Prandtl number of optimum biodiesel from food industrial waste oil and diesel fuel blend for diesel engine. Fuel. 285: 119049. doi.org/10.1016/j.fuel.2020.119049

Samuel, O.D., Okwu, M.O., Tartibu, L.K., Giwa, S.O., Sharifpur, M., Jagun, Z.O.O. 2021. Modelling of *Nicotiana Tabacum L.* oil biodiesel production: Comparison of ANN and ANFIS. Front. Energy Res. 8: 612165. doi.org/10.3389/fenrg.2020.612165

Tang, Z.E., Lim, S., Pang, Y.L., Ong, H.C., Lee, K.T. 2018. Synthesis of biomass as heterogeneous catalyst for application in biodiesel production: State of the art and fundamental review. Renew. Sustain. Energy. Rev. 92: 235–253. doi.org/10.1016/j.rser.2018.04.056

Tang, Z.E., Lim, S., Pang, Y.L., Shuit, S.H., Ong, H.C. 2020. Utilisation of biomass wastes based activated carbon supported heterogeneous acid catalyst for biodiesel production. Renew. Energ. 158: 91–102. doi.org/10.1016/j.renene.2020.05.119

Upretym, B.K., Chaiwong, W., Ewelike, C., Rakshit, S.K. 2016. Biodiesel production using heterogeneous catalysts including wood ash and the importance of enhancing byproduct glycerol purity. Energ. Convers. Manage. 115: 191–199. doi.org/10.1016/j.enconman.2016.02.032

Tshizanga, N., Aransiola, E.F., Oyekola, O. 2017. Optimisation of biodiesel production from waste vegetable oil and eggshell ash. S. Afr. J. Chem. Eng. 23: 145–156. doi.org/10.1016/j.sajce.2017.05.003

Wadood, A., Rana, A., Basheer, C., Razzaq, S.A., Farooq, W. 2020. *In situ* transesterification of microalgae *Parachlorella kessleri* biomass using sulfonated rice husk solid catalyst at room temperature. Bioenerg. Res. 13: 530–541. doi.org/10.1007/s12155-019-10060-3

Wang, S., Zhao, C., Shan, R., Wang, Y., Yuan, H. 2017. A novel peat biochar supported catalyst for the transesterification reaction. Energ. Convers. Manage. 139: 89–96. doi.org/10.1016/j.enconman.2017.02.039

Xue, M., Chen, C., Ren, Z., Tan, Y., Li, B., Zhang, C. 2017. A novel mangosteen peels derived hierarchical porous carbon for lithium sulfur battery. Mater. Lett. 209: 594–597. doi.org/10.1016/j.matlet.2017.08.090

Yahya, S., Wahab, S.K.M., Harun, F.W. 2020. Optimization of biodiesel production from waste cooking oil using Fe-Montmorillonite K10 by response surface methodology. Renew. Energ. 157: 164–172. doi.org/10.1016/j.renene.2020.04.149

Yang, R., Guo, X., Jia, L., Zhang, Y., Zhao, Z., Lonshakov, F. 2017. Green preparation of carbon dots with mangosteen pulp for the selective detection of Fe^{3+} ions and cell imaging. Appl. Surf. Sci. 423: 426–432. doi.org/10.1016/j.apsusc.2017.05.252

Zhao, C., Lv, P., Yang, L., Xing, S., Luo, W., Wang, Z. 2018. Biodiesel synthesis over biochar-based catalyst from biomass waste pomelo peel. Energ. Convers. Manage. 160: 477–485. doi.org/10.1016/j.enconman.2018.01.059